

**PREPARATION OF MAPS DEPICTING GEOTHERMAL
GRADIENT AND PRECAMBRIAN STRUCTURE IN THE
PERMIAN BASIN**

By

Stephen C. Ruppel, Rebecca H. Jones, Caroline L. Breton, and Jeffrey A. Kane

Bureau of Economic Geology
Jackson School of Geosciences
The University of Texas at Austin
Austin, TX 78713-8924

Contract report to the U.S. Geological Survey
Order no. 04CRSA0834 and requisition no. 04CRPR01474
May 12, 2005

Contents

SUMMARY	1
INTRODUCTION	1
PERMIAN BASIN BASEMENT STRUCTURE MAP	2
Background	2
Methodology	5
<i>Construction of Ellenburger Structure Map</i>	5
<i>Construction of Precambrian Structure Map</i>	7
Data Presentation	8
PERMIAN BASIN GEOTHERMAL GRADIENT MAP	9
Introduction	9
Methodology	10
<i>Equilibrium correction</i>	12
<i>Geothermal gradient calculation</i>	12
<i>Data smoothing and gridding</i>	13
<i>Grid import and contouring</i>	17
Data Presentation	17
ACKNOWLEDGMENTS	19
REFERENCES	20
APPENDIX (IN POCKET): DATA CD	22

Figures

1. Map of the Permian Basin study area showing areas where different surfaces were contoured by Ewing (1990)	3
2. Simplified stratigraphic column showing formations and their related periods and epochs	4
3. Permian Basin study area	11
4. Plot of geothermal gradient versus well depth	14
5. Comparison of three different search radius options for map smoothing	16

Tables

1. Excerpt from the table of digitized well data from the Tectonic Map of Texas (Ewing, 1990) to show contents and the abbreviations used..... 6
2. Excerpt from the Precambrian well data table to show contents and the abbreviations used 8
3. Computed data used for outlier identification in the depth domain..... 15
4. Excerpt from the well data table to show contents and the abbreviations used 18

SUMMARY

Maps depicting (1) regional trends in geothermal gradient and (2) the structure of the top of the Precambrian basement were prepared for the Permian Basin area. Both maps, along with supporting data, were integrated in a Geographic Information System (GIS) project.

INTRODUCTION

The objectives of this project were to prepare maps depicting (1) the geothermal gradients, and (2) the structure on the top of the Precambrian in the Permian Basin of West Texas and New Mexico. Both were to be created and distributed in a spatially related Geographic Information System (GIS) project.

The preparation of these maps involved two different sets of issues. Prior to this study, no publicly available, detailed map of Precambrian structure with referenced control points existed for the Permian Basin. This is in part a function of the sparsity of data (Precambrian well penetrations) and in part a function of the lack of interest in assembling such a map. Additionally, no digital, GIS-based map of Precambrian structure was previously available. To prepare this map over the entire area of interest, it was necessary to develop new creative approaches.

By contrast, more than one map depicting geothermal gradient has been previously published. Additionally, relatively extensive data sets of bottom-hole well temperatures are available. The issues in preparing this map revolve around (1) deciding what data to use, (2) developing ways to deal with possible errors in the data, and (3) making proper corrections to the data.

The details of the procedures used to produce each map are presented below.

PERMIAN BASIN BASEMENT STRUCTURE MAP

Background

Construction of basement structure maps in the Permian Basin is inherently difficult using well data owing to the paucity of Precambrian well penetrations. As a result, very few maps of Precambrian structure in the Permian Basin have been published. One of these, presented in Frenzel and others (1988), lacks well control or reference to the data source. By contrast, numerous maps have been previously published on the Lower Ordovician structure in conjunction with studies of the Lower Ordovician (Ellenburger) production. These include maps presented by Galley (1958), the Texas Water Development Board (1972), Wright (1979), Frenzel and others (1988), and, most recently, Ewing (1990). Given this situation, we chose an innovative approach to create a detailed representation of the structure of the Precambrian that utilizes the relative abundance of information about the overlying section.

Although the Tectonic Map of Texas (Ewing, 1990) does not provide a map of Precambrian basement structure, it is one of the few published maps to incorporate both well data and modern fault interpretations in a detailed mapping of Ellenburger (Lower Ordovician) structure over the Permian Basin region. This map provides a synthesis of structural interpretations supported by widely distributed surface and subsurface data (more than 4,000 control points in the Permian Basin). Basement faults are mapped in detail, and 200-m structural contours are mapped on the top of the Lower Ordovician Ellenburger and Arbuckle Groups in most places (Figure 1) and in some areas (New Mexico and a small part of westernmost Texas as shown in Figure 1) on the top of the "Siluro-Devonian carbonate" (essentially the base of Upper Devonian Woodford Formation; Figure 2). Where the Precambrian subcrops (Figure 1), the Ellenburger structural contours are on the subcrop surface.

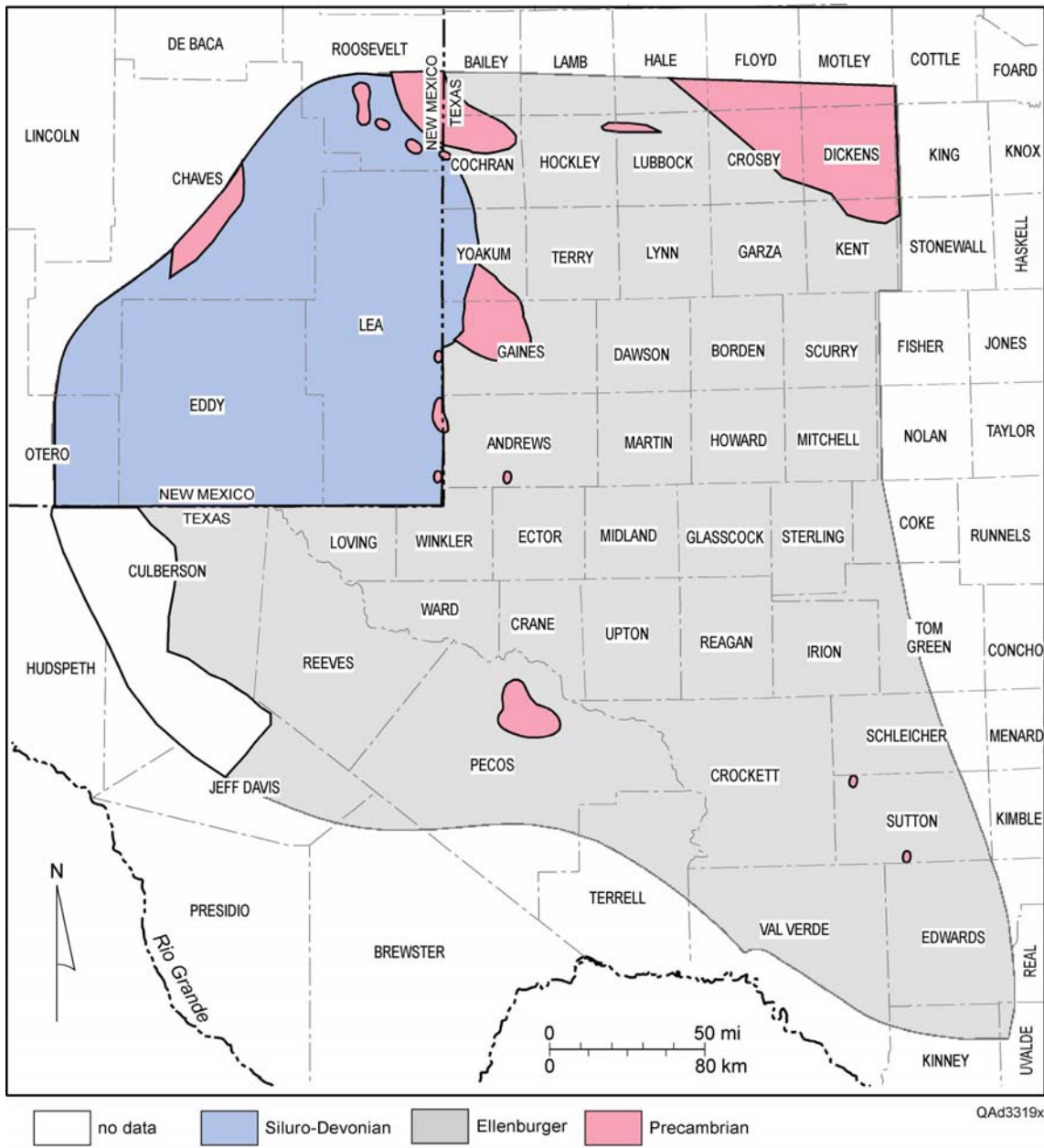


Figure 1. Map of the Permian Basin study area showing areal distribution of contouring datums used by Ewing (1990).

System	Epoch/Series/Stage	Time (m.y.)	New Mexico	Texas				
	Kinderhookian	363	Woodford	Woodford				
DEVONIAN	Famennian		[Vertical lines]	[Vertical lines]	[Vertical lines]			
	Frasnian							
	Givetian							
	Eifelian							
	Emsian							
	Pragian					Thirtyone	Thirtyone	
	Lochkovian					417	Wristen Group	Fasken
Pridoli	Wink							
Ludlovian	[Vertical lines]	[Vertical lines]						
Wenlock								
Llandovery	443	Fusselman	Fusselman					
ORDOVICIAN		Ashgill	Montoya	Sylvan	Montoya			
		Caradoc	Simpson Group	Bromide	Tulip Creek	McLish	Oil Creek	Joins
		Llandeilo						
		Llanvirn						
		Arenig		Ellenburger	Ellenburger			
		Tremadoc						
		CAMBRIAN		495	Bliss	Cambrian		
	Cambrian							
PRECAMBRIAN								

Figure 2. Stratigraphic column of lower Paleozoic strata in the Permian Basin region. Modified from Dutton and others (2004).

Methodology

Because well-bore penetrations of the Precambrian are relatively few, we used the Tectonic Map of Texas (Ewing, 1990) as a primary source in constructing a basement map for the Permian Basin. Our basic approach was to start with the detailed structural horizons provided by this map and use published thickness maps to extrapolate the structure to the Precambrian basement. Details of the procedure are given below.

Construction of Ellenburger Structure Map

Structural contours were first scanned for the Permian Basin region from the Tectonic Map of Texas (Ewing, 1990). We scanned both the published map (Ewing, 1990), which is contoured in metric units (meters below sea level), and work versions of the map, which are contoured in English units (feet below sea level); the latter were provided by the author for use in our study. All contour and fault trace data were then used to produce spatially registered GIS shape files. Well locations and stratigraphic tops (Ellenburger, Precambrian, and “Siluro-Devonian”) from well and outcrop control were also digitized and converted into a shape file (Table 1).

Because structure on the Tectonic Map of Texas (Ewing, 1990) was contoured on the top of “Siluro-Devonian” (base of the Woodford) over a small part of the study area (dominantly in New Mexico, see Figure 1) rather than on the Ellenburger, it was first necessary to extend Ellenburger contours to this area. To do this, we scanned and gridded published thickness maps of the intervening section, which consists of the Middle and Upper Ordovician and Silurian-Devonian (Figure 2). For the thickness of the Middle Ordovician (Simpson Group) and the Silurian-Devonian we used recent revised versions of Galley’s map (Galley, 1958, published in Frenzel and others, 1988). For the Upper Ordovician thickness we used the Montoya/Maravillas/Sylvan isopach published by Wright (1979). The digital grids from all three maps were summed. This summed thickness was subtracted from the contoured “Siluro-Devonian” surface (in feet below sea level) where it was mapped by Ewing (1990) (Figure 1)

to create the deeper Ellenburger structural contours. These newly created Ellenburger contours were then seamed with the Ellenburger contours from the original Tectonic Map of Texas (Ewing, 1990) to create a complete map of top Ellenburger structure in feet below sea level across the entire Permian Basin area.

Table 1. Excerpt from the table of digitized well data from the Tectonic Map of Texas (Ewing, 1990) to show contents and abbreviations used. From left, columns are point identification number (ID), formation (FORMATION), depth of formation top in feet below sea level (DEPTH_FT) data source (SOURCE), and approximate X and Y locations of the digitized data point (XCOORD and YCOORD).

ID	FORMATION	DEPTH_FT	SOURCE	XCOORD	YCOORD
1	Precambrian	-1797	digitized from Tectonic Map of Texas (Ewing, 1990)	-125819.4560	652853.5733
2	Precambrian	-2030	digitized from Tectonic Map of Texas (Ewing, 1990)	418012.8783	-187910.1933
3	Precambrian	-2180	digitized from Tectonic Map of Texas (Ewing, 1990)	373691.3764	-200482.6333
4	Precambrian	-2362	digitized from Tectonic Map of Texas (Ewing, 1990)	-89282.8465	687707.3358
5	Precambrian	-2515	digitized from Tectonic Map of Texas (Ewing, 1990)	138809.1894	870974.3091
6	Precambrian	-2570	digitized from Tectonic Map of Texas (Ewing, 1990)	420538.3730	-203932.2533
7	Precambrian	-2690	digitized from Tectonic Map of Texas (Ewing, 1990)	128537.7451	884032.6926
8	Precambrian	-2880	digitized from Tectonic Map of Texas (Ewing, 1990)	389479.4362	-204807.5617
9	Precambrian	-3221	digitized from Tectonic Map of Texas (Ewing, 1990)	248536.9466	886989.6204
10	Precambrian	-3225	digitized from Tectonic Map of Texas (Ewing, 1990)	186935.5030	902458.5636
11	Precambrian	-3327	digitized from Tectonic Map of Texas (Ewing, 1990)	14130.7636	787868.8717
12	Precambrian	-3500	digitized from Tectonic Map of Texas (Ewing, 1990)	352889.1154	802220.2002
13	Precambrian	-3512	digitized from Tectonic Map of Texas (Ewing, 1990)	179748.7683	835081.4520
14	Precambrian	-3514	digitized from Tectonic Map of Texas (Ewing, 1990)	220311.0332	896122.1955
15	Precambrian	-3598	digitized from Tectonic Map of Texas (Ewing, 1990)	168310.0683	835737.1078
16	Precambrian	-3697	digitized from Tectonic Map of Texas (Ewing, 1990)	181331.5511	812535.1183
17	Precambrian	-3701	digitized from Tectonic Map of Texas (Ewing, 1990)	149376.8583	878140.0483
18	Precambrian	-3716	digitized from Tectonic Map of Texas (Ewing, 1990)	263709.8523	318137.0778
19	Precambrian	-3730	digitized from Tectonic Map of Texas (Ewing, 1990)	221230.2425	779811.1437
20	Precambrian	-3969	digitized from Tectonic Map of Texas (Ewing, 1990)	294000.4042	797752.4989

Construction of Precambrian Structure Map

The Precambrian structure map was created by subtracting the thickness of the Lower Ordovician–Cambrian section from the contoured Ellenburger structural surface. We deemed the best map of the thickness of the Lower Ordovician–Cambrian section to be the map compiled and published by the Texas Water Development Board (1972). However, because this map does not extend to New Mexico, a Lower Ordovician–Cambrian thickness map published by Wright (1979) was used for New Mexico. Again, these maps were scanned, gridded, and merged and then subtracted from the Ellenburger structure map to generate a map of the structure of the Precambrian surface in feet below sea level. The Precambrian map was contoured without faults, and then the Tectonic Map of Texas (Ewing, 1990) faults were overlain on the map. This procedure resulted in tightly spaced contours paralleling faults, rather than contour terminations at faults.

We refined the Precambrian structure map we created by extrapolation from the Ellenburger by comparing structural contours with a set of approximately 360 Precambrian well penetrations in the region and modifying them as necessary (Table 2). We compiled these wells from publications, digital well data sets, and data collected by other researchers. Locations for these wells were matched to API numbers, and the complete set was then loaded as a shape file.

Table 2. Excerpt from the Precambrian well data table to show contents and the abbreviations used. From left, columns are API well identification number (API), latitude and longitude in decimal degrees (LAT, LONG), total depth in feet measured (TD_FT_MD), total depth in feet below sea level (TDFTSUBSEA), formation at total depth (FM_AT_TD), top of basement in feet measured (TBASE_MD) and in feet below sea level (TBASESUBSE) where available, operator name (OP_NAME), lease/well name (WELL_NAME), and well number (WELL_NO).

API	LAT	LONG	TD_FT_MD	TDFTSUBSEA	FM_AT_TD	TBASE_MD	TBASESUBSE	OP_NAME	WELL_NAME	WELL_NO
300050001800	32.99086	-104.78599	5849	-1681	Precambrian			HUMBLE OIL & REFINING	GORMAN-FED	1
300050009600	33.26870	-104.43341	5828	-2265	Precambrian			FRANKLIN-ASTON & FAIR	ORCHARD PARK	1
300050009800	33.21008	-104.47229	5502	-1909	Precambrian			DELTA DRLG	CLAYTON	1
300050010700	33.00640	-104.41045	7722	-4302	Precambrian			MAGNOLIA PET	RALPH O PEARSON	1
300050011600	33.07593	-104.32026	8389	-4976	Precambrian			MAGNOLIA PET	MC BROWN	1
300050012300	33.36676	-104.29120	6129	-2507	Precambrian			RICHFIELD OIL	COMANCHE UNIT	1
300050017200	33.33751	-104.31712	6175	-2506	Precambrian			BUFFALO OIL ETAL	COMANCHE UNIT	3
300050019900	33.05415	-104.20786	9983	-6455	Precambrian			CITIES SERVICE OIL	BAETZ A	1
300050024600	33.44034	-104.19180	7215	-3354	Precambrian			SWEENEY H N	DIABLO STATE	1
300050025100	33.40752	-104.22647	6930	-3207	Precambrian			SINCLAIR OIL	STATE-CHAVES 180	1
300050027400	33.36316	-104.18788	6933	-3170	Precambrian			PAN AMERICAN	STATE C F	1
300050030200	33.36294	-104.27422	6630	-2957	Precambrian			RICHFIELD OIL	LILLIAN COLL	1
300050031600	33.35592	-104.19199	7315	-3566	Precambrian			HONOLULU OIL	FED-HINKLE	1
300050032000	33.33423	-104.22644	7582	-3791	Precambrian			UNION OIL-DEKALB	STATE OF NEW MEXICO	1
300050032800	33.31973	-104.23938	7430	-3736	Precambrian			HUMBLE OIL & REFINING	STATE Y	1
300050034500	33.48421	-104.13560	7463	-3575	Precambrian			DEKALB PET & MAGNOLIA	JP WHITE UNIT	1
300050040300	33.65774	-103.93444	8731	-4545	Precambrian			MAGNOLIA PET	STATE Z	1
300050040500	33.83545	-103.84800	8911	-4572	Precambrian			SPARTAN DRLG CO	STATE 25	1
300050040700	33.65057	-104.02578	7390	-3362	Precambrian			HAMON JAKE L	N SALISBURY	1
300050042100	33.30123	-104.07097	9058	-5348	Precambrian			RICHFIELD OIL	JP WHITE	1

Data Presentation

Project deliverables for the Precambrian structure mapping part of the study include the following:

1. A structure map of contours on the top of the Precambrian in the Permian Basin area in feet below sea level.

2. A structure map of contours on the top of the Ellenburger in the Permian Basin area in feet below sea level.
3. Well data shape file of wells used in mapping. These include both those digitized from the Tectonic Map of Texas and the Precambrian well penetrations collected during this study.
4. Stratigraphic tops on "Siluro-Devonian," Ellenburger, and Precambrian where available.

PERMIAN BASIN GEOTHERMAL GRADIENT MAP

Introduction

The goal of this task was to create a map depicting variations in geothermal gradient and distribute the data and map in GIS. To accomplish this, we examined numerous previous geothermal gradient maps as potential data sources.

The most recent work on geothermal heat flow is that of Blackwell and others at the Southern Methodist University (SMU) Geothermal Laboratory. These workers have recently updated maps originally produced as part of the Geological Society of America's Decade of North American Geology (Blackwell and Steele, 1992) and published them as the Geothermal Map of North America (Blackwell and Richards, 2004a, b). The focus of this map is the integration of heat flow and geothermal gradient data across the entire continent.

Woodruff (1982) produced a map specifically focused on central and northern Texas, but data density in the Permian Basin area is very sparse.

Perhaps, the most comprehensive and valuable data set available is the set of contoured geothermal gradient maps generated by the Geothermal Survey of North America (GSNA) for all of North America, including the Permian Basin, in 1970. These data and maps were published by the American Association of Petroleum Geologists (AAPG) in 1972, and most recently the data have been made available on CD in ASCII format (AAPG DataRom, 1994). The GSNA data

set contained on the CD is a primary source for the aforementioned maps generated by the SMU Geothermal Laboratory. Data from this project include API well identification numbers, latitude, longitude, measured bottom-hole temperatures, depth of measurement, and average surface temperature by state and county.

Methodology

Most workers have applied an equation-based correction to raw bottom-hole temperatures to account for nonequilibrium conditions before calculating geothermal gradient or heat flow. The corrected gradients have then generally been smoothed before contouring to generate maps. Unfortunately, many previously prepared maps either do not fully describe the corrections used (e.g., GSNA, 1970) or use coarse contouring intervals and smoothing procedures that are only appropriate for less detailed maps (e.g., the Geothermal Map of North America [Blackwell and Richards, 2004b]). Both to honor currently accepted methods and to preserve the detail desired for the Permian Basin area, we used the data set and equilibrium correction employed by the SMU Geothermal Laboratory in the creation of the 2004 Geothermal Map of North America but smoothed and contoured data at a finer scale.

The SMU Geothermal Laboratory provided us with their geothermal database for the Permian Basin. This database includes basic well data and the deepest measured bottom-hole temperature from the GSNA (AAPG DataRom, 1994). They filtered GSNA data to eliminate shallow measurements (less than 600 m [1,969 ft]) and then applied an equilibrium correction and depth-specific smoothing. We found that their definition of the Permian Basin was slightly smaller than ours (Figure 3), so we retrieved data for a few additional counties from the original GSNA source (AAPG DataRom, 1994). Unfortunately, data for Lea and Eddy Counties in New Mexico were not available from either source. We then applied the equilibrium correction used by the SMU Geothermal Laboratory (from Harrison, 1983) to bottom-hole temperature measurements to account for nonequilibrium conditions. The difference between corrected bottom-hole and

surface temperatures was then divided by depth to yield geothermal gradient. To make this calculation, we chose to use surface temperatures based on average annual surface temperature reported by the GSNA (AAPG DataRom, 1994) rather than those based on surface-water temperatures (from Gass, 1982) that were used by SMU. Finally, we filtered and smoothed the data with respect to depth and geographic distribution and generated a grid for contouring over the study area.

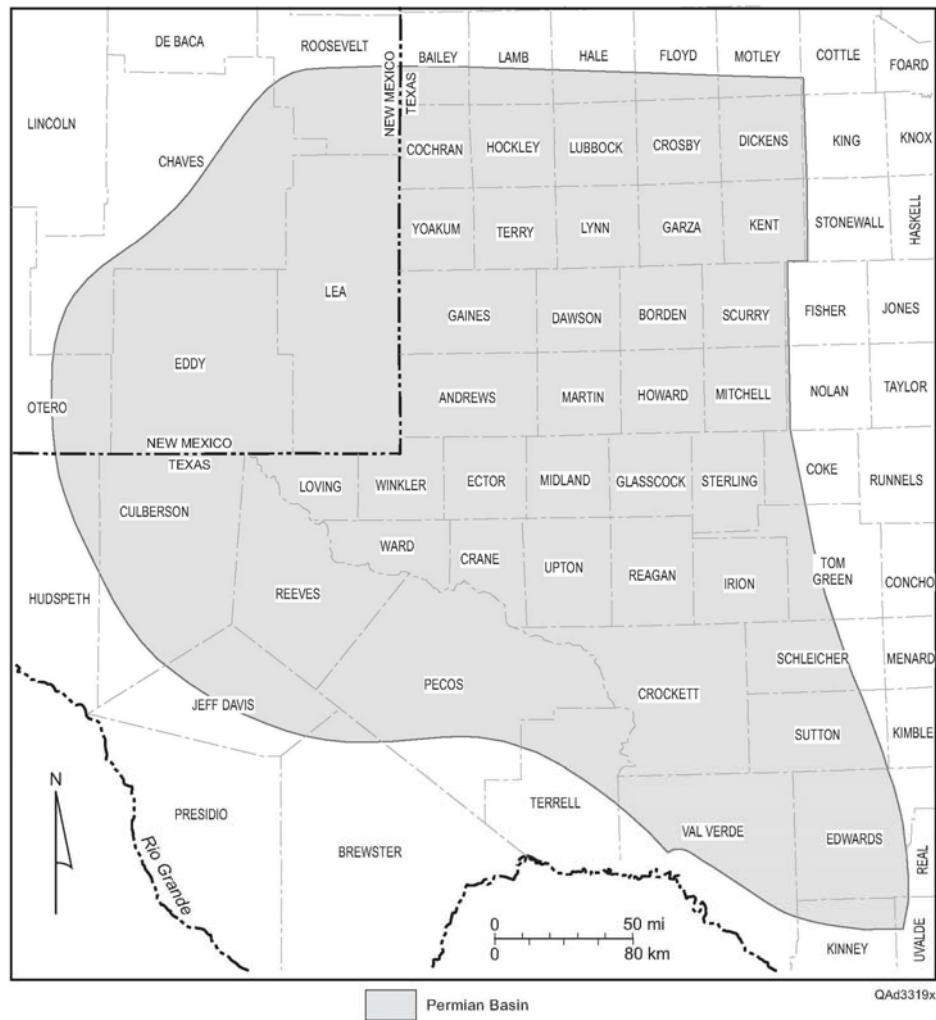


Figure 3. Permian Basin study area.

Equilibrium correction

Bottom-hole temperature (BHT) measured at the well bore is problematic in that the temperature recorded may not reflect a true equilibrium temperature owing to differences between the temperature of the rock and that of the circulating fluid. To better understand this problem, early geothermal workers (Kehle and others, 1970; Schoepel and others, 1970) studied drill pipe fluid, annulus fluid, borehole wall, and formation temperatures as a function of circulation time and depth. They also studied the effects of cessation of drilling, depth, and radial distance of the formation from the well bore on temperature. The difference between typical BHT readings and true equilibrium temperatures was found to be a function of depth, and empirical corrections were derived for specific data sets.

Since that time, other workers have compared BHT measurements with drill-stem tests and derived more universal empirical corrections. A correction generated from drill-stem test data in Oklahoma by Harrison and his students (Harrison and others, 1983; Cheung, 1978) was applied to construct the recent Geothermal Map of North America (2004) and has been used in the past by other workers in Texas (e.g., Ruppel, 1985). We applied the Harrison (1983) correction as derived by the SMU Geothermal Laboratory to the Permian Basin BHT as follows:

$$\text{Corrected BHT (}^{\circ}\text{C)} = -16.51213476 + (0.01826842109 * \text{measured BHT}) - 0.000002344936959 * (\text{measured BHT})^2$$

Geothermal gradient calculation

To calculate geothermal gradient, we divided corrected bottom-hole temperature by surface temperature. As stated above, we chose to use the average annual surface temperatures reported by the GSNA (AAPG DataRom, 1994). The surface-water temperatures from Gass (1982) are less accurate

because they are extrapolated over the Permian Basin region. The GSNA data showed good agreement with other sources of surface temperatures.

Geothermal gradient = (Corrected BHT – surface temperature)/depth

Data smoothing and gridding

After calculating the geothermal gradient for all wells in the study area, several steps were taken to filter and smooth the data to generate grids for contouring. There are many sources of possible error associated with reported bottom-hole well temperatures, in addition to those addressed by the equilibrium correction. Among these are (a) faulty or inaccurate thermometers, (b) operator error, (c) errors in recording or transcription, and (d) errors in well locations. All of these errors are for statistical purposes random and nearly impossible to specifically identify. A key goal of this operation was to remove or reduce the impact of random errors in mapping of geothermal gradients.

A review of the data suggests that the individual gradient value associated with a well has a magnitude defined by two attributes—the first attribute associated with the total depth of the well and the second associated with its location areally. This means that errors, or noise, in the data can occur in both the depth (z) domain and in the areal (x–y) domain. In order to identify and reject possible erroneous data, or outliers, we assumed that these two domains are independent. Working from this assumption, two methods were used to eliminate outliers from the data. The first step, rejection in the depth domain, was handled in a manner similar in structure to computing semi-averages. The data set was divided up into 500-ft subpopulations, i.e., intervals from 2,500 to 3,000 ft, 3,000 to 3,500 ft, etc. The average and standard deviation of the data in each of these intervals was then computed. The actual data and the computed semi-averages are shown graphically in Figure 4. The averages, standard deviations, and rejection criteria are given in Table 3.

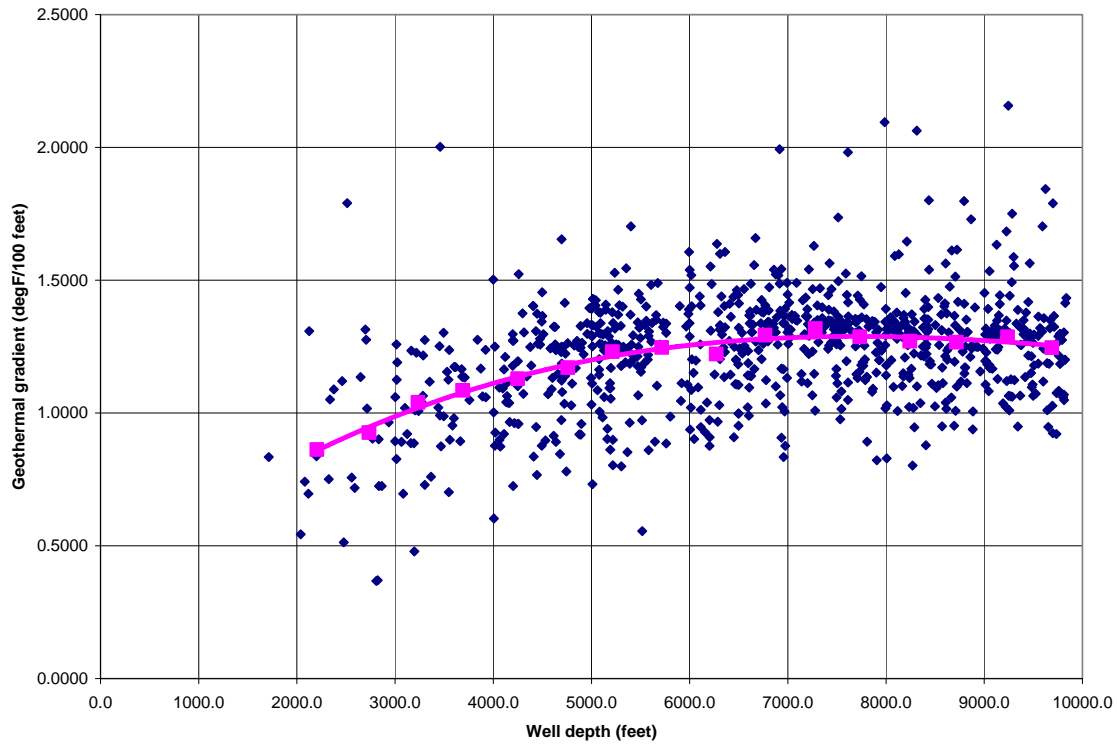


Figure 4. Plot of geothermal gradient versus well depth. Geothermal data have been computed using the bottom-hole temperature data with Harrison corrections applied and surface temperature data from the AAPG DataRom (1994). Blue points are individual data values. Magenta points are computed averages for 500-ft-depth intervals. The magenta connecting line indicates the trend only.

Data were rejected if more than two standard deviations away from the mean. A total of 32 data points, or 9% of the data, were rejected as being outside of the two-standard-deviation limits. Their rejection reduced the data set from 852 data points to 820 data points.

Table 3. Computed data used for outlier identification in the depth domain. The rightmost two columns are the minimum and maximum values considered acceptable for that depth interval. These two columns are defined as the mean minus two standard deviations for the minimum and the mean plus standard deviations for the maximum. All data less than the minimum or greater than the maximum were rejected as outlier data.

TOP DEPTH OF INTERVAL	BASE DEPTH OF INTERVAL	AVERAGE DEPTH OF INTERVAL	AVERAGE GRADIENT OF INTERVAL	STANDARD DEVIATION OF GRADIENT DATA	AVERAGE GRADIENT -2 (AVERAGE) STANDARD DEVIATIONS	AVERAGE GRADIENT + 2 (AVERAGE) STANDARD DEVIATIONS
0	2500	2204.4	0.8624	0.2515	0.4572	1.2676
2500	3000	2735.3	0.9261	0.3771	0.5209	1.3313
3000	3500	3234.1	1.0400	0.2632	0.6348	1.4452
3500	4000	3689.2	1.0854	0.1369	0.6802	1.4907
4000	4500	4248.5	1.1292	0.2103	0.7239	1.5344
4500	5000	4759.0	1.1712	0.1689	0.7660	1.5764
5000	5500	5214.7	1.2307	0.1819	0.8254	1.6359
5500	6000	5716.5	1.2467	0.2113	0.8414	1.6519
6000	6500	6271.9	1.2221	0.2029	0.8168	1.6273
6500	7000	6767.6	1.2932	0.1820	0.8880	1.6984
7000	7500	7278.8	1.3178	0.1119	0.9126	1.7231
7500	8000	7731.5	1.2871	0.1909	0.8819	1.6923
8000	8500	8242.8	1.2708	0.1835	0.8655	1.6760
8500	9000	8716.8	1.2670	0.1815	0.8618	1.6722
9000	9500	9239.6	1.2875	0.1901	0.8823	1.6928
9500	10000	9687.9	1.2462	0.1979	0.8410	1.6514

Analysis for outliers in the areal or x - y domain was accomplished by computing a moving average across the remaining data set after outlier rejection in the depth domain. Several different search radii were computed from 20,000 to 200,000 ft and compared to determine an optimal search radius. Optimal in this case implies a search that is large enough so that local perturbations such as outlier data are suppressed but longer order trends are retained. A visual comparison of the maps created using different scale factors resulted in a choice of a 100,000-ft scale factor. The 100,000-ft scale factor appeared to give a reasonable tradeoff between outlier suppression without significant loss of gradient variability. Example maps at three different search radii are shown in Figure 5.

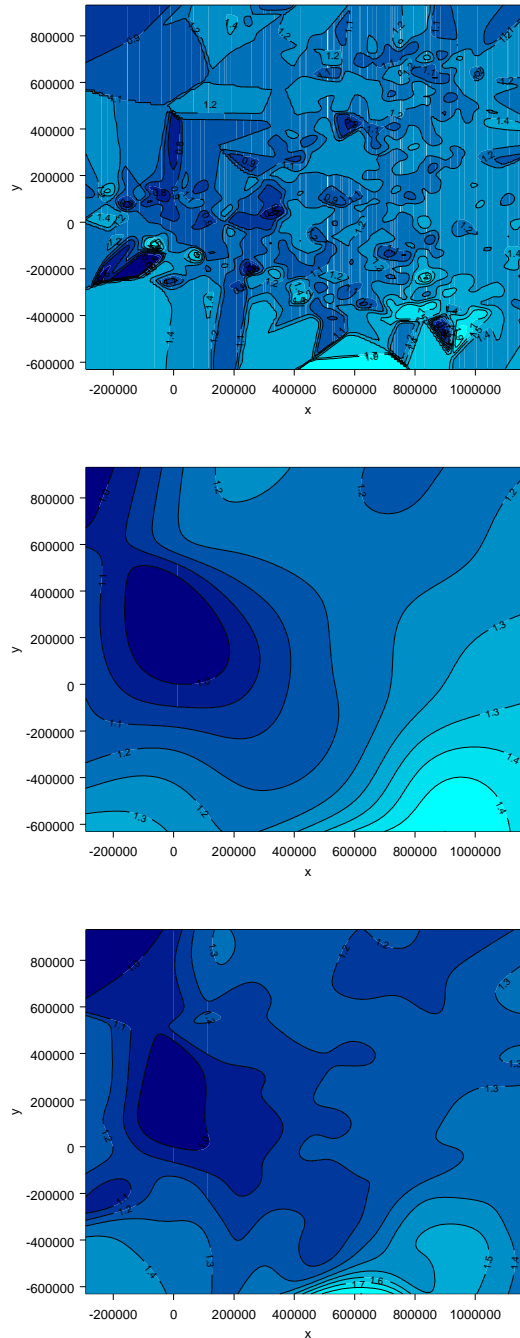


Figure 5. Comparison of three different search radius options for map smoothing. The upper map was created with a search radius of 25,000 ft. Note the large number of artifacts or “bull’s eyes” indicating that the search radius is too small to effectively suppress noisy data. The middle map was created using a search radius of 200,000 ft. Note that only the long period trend is apparent. The bottom map was created with a 100,000-ft search radius. It provides a good balance between the two extremes.

Once a scale factor choice was made, an average value was computed at each well location using the 100,000-ft scale factor and compared with the actual datum value at the well location. The standard deviation of the differences between the measured and averaged values was computed, and a two-standard-deviation rejection criterion was again used to eliminate outlier data. This was accomplished by assuming that the locally computed average, using a 100,000-ft search radius, was the correct value at that well location. The actual datum value was compared with that averaged value. If the actual datum was different from the smoothed value by more than two standard deviations it was rejected as an outlier. This resulted in an additional 34 data points being rejected using the areal outlier argument.

The remaining 786 data points were then used to create a grid of smoothed data, again using the 100,000-ft search radius to compute the moving average.

Grid import and contouring

The smoothed grid nodes and associated data were imported into GIS software and converted to a point shape file. A grid was created from these points using the spatial analysis tool and the inverse distance-weighted technique. This grid was then contoured every 0.01°F/100 ft. The equilibrium-corrected but unsmoothed geothermal gradient values from each well were then compared with the contours.

Data Presentation

Project deliverables for the geothermal gradient part of the study contain the following:

1. A gridded, smoothed geothermal gradient map for the Permian Basin area contoured every 0.01°F/100 ft. It will be noted that map coverage does not extend into Eddy and Lea Counties, New Mexico. This is due to the lack of available well data and bottom-hole temperature data in that area. Note that the map values of the smoothed map do not necessarily agree with well values.

2. A contour map of corrected but unsmoothed data contoured every 0.1°F/100 ft. This map honors original well values. As such, it displays many bull's eyes resulting from individual high and low values that are apparent even at this coarser contour interval.
3. Well data shape files of wells used to generate the two contour maps. Well data tables include API well identification number (API_NO), latitude and longitude in decimal degrees (LAT_DD, LONG_DD), depth of measurement in feet and meters (DPTH_FT, DPTH_M), equilibrium-corrected geothermal gradient in degrees Fahrenheit per 100 ft (IGGF100FT) and degrees Celsius per kilometer (IGG_CKM), and smoothed geothermal gradient in degrees Fahrenheit per 100 ft (FGGF100FT) as shown in Table 4.

Table 4. Excerpt from the well data table to show contents and the abbreviations used. From left, columns are API well identification number (API_NO), latitude and longitude in decimal degrees (LAT_DD, LONG_DD), depth of measurement in feet and meters (DPTH_FT, DPTH_M), equilibrium-corrected geothermal gradient in degrees Fahrenheit per 100 ft (IGGF100FT) and degrees Celsius per kilometer (IGG_CKM), and smoothed geothermal gradient in degrees Fahrenheit per 100 ft (FGGF100FT).

API_NO	LAT_DD	LONG_DD	DPTH_FT	DPTH_M	IGGF100FT	IGG_CKM	FGGF100FT
424350022200	30.2860	-100.5990	6851	2088	1.34	24.35	1.39
421051062700	30.2890	-101.2060	5994	1827	1.61	29.27	1.42
424350027700	30.2970	-100.2150	4979	1518	1.40	25.43	1.36
421051096400	30.3230	-101.3710	5573	1699	1.20	21.90	1.40
424430004200	30.3310	-101.7780	5965	1818	1.33	24.17	1.37
424350020800	30.3370	-100.3170	5299	1615	1.23	22.49	1.36
424350013500	30.3450	-100.3540	5607	1709	1.48	27.03	1.37
424433000600	30.3570	-101.7040	6103	1860	1.44	26.24	1.38
424353001200	30.3930	-100.2370	4200	1280	1.27	23.20	1.35
424351028500	30.4020	-100.5290	5558	1694	1.35	24.55	1.39
424430006500	30.4080	-101.9060	6307	1922	1.31	23.96	1.31
424351004300	30.4100	-100.3030	5140	1567	1.25	22.85	1.36
421051076700	30.4130	-101.6540	7424	2263	1.56	28.50	1.37
424350019100	30.4140	-100.4250	5482	1671	1.45	26.41	1.37
424350026000	30.4310	-100.6280	6022	1835	1.40	25.55	1.41
424351005500	30.4500	-100.8280	9463	2885	1.56	28.51	1.43
424431020100	30.4680	-101.9090	7913	2412	1.26	23.04	1.30
424351003900	30.4720	-100.4790	5317	1621	1.40	25.53	1.38
424350011200	30.4750	-100.1670	4260	1299	1.52	27.75	1.34

ACKNOWLEDGMENTS

This report was funded by the U.S. Geological Survey, under order no. 04CRSA0834 and requisition no. 04CRPR01474.

We gratefully acknowledge Melanie Barnes of Texas Tech University for providing well data for Precambrian basement penetrations; Tom Ewing for providing work copies of the Tectonic Map of Texas; and Maria Richards of the SMU Geothermal Laboratory for providing geothermal data and an explanation of the Laboratory's methodology. Editing was by Susann V. Doenges.

REFERENCES

- American Association of Petroleum Geologists, 1994, DataRom (CSDE, COSUNA, and GSNA) 1994: Tulsa, Oklahoma, AAPG/Datapages: CD.
- Blackwell, D. D., and Richards, M., 2004a, Calibration of the AAPG Geothermal Survey of North America BHT Data Base: American Association of Petroleum Geologists Annual Meeting 2004, Dallas, Texas, Poster session, paper 87616.
- Blackwell, D. D., and Richards, M., eds., 2004b, Geothermal map of North America: American Association of Petroleum Geologists, Tulsa, Oklahoma.
- Blackwell, D. D., and Steele, J. L., 1992, Geothermal map of North America: Denver, Colorado, Geological Society of America, Decade of North American Geology.
- Cheung, P. K., 1978, The geothermal gradient in sedimentary rocks in Oklahoma: University of Oklahoma, Ph.D. dissertation, 116 p.
- Ewing, T. E., 1990, Tectonic map of Texas: The University of Texas at Austin, Bureau of Economic Geology, 4 sheets, scale 1: 750,000.
- Dutton, S. P., Kim, E. M., Broadhead, R. F., Breton, C. L., Raatz, W. D., Ruppel, S. C., and Kerans, C., 2004, Play analysis and digital portfolio of major oil reservoirs in the Permian Basin: application and transfer of advanced geological and engineering technologies for incremental production opportunities: The University of Texas at Austin, Bureau of Economic Geology, and New Mexico Bureau of Geology and Mineral Resources, New Mexico Institute of Mining and Technology, annual report prepared for U.S. Department of Energy, under contract no. DE-FC26-02NT15131, 104.
- Frenzel, H. N., Bloomer, R. R., Cline, R. B., Cys, J. M., Galley, J. E., Gibson, W. R., Hills, J. M., King, W. E., Seager, W. R., Kottowski, F. E., Thompson, S., III, Luff, G. C., Pearson, B. T., and Van Siclen, D. C., 1988, The Permian Basin region, *in* Sloss, L. L., ed., Sedimentary cover— North American Craton; U.S.: Boulder, Colorado, Geological Society of America, The Geology of North America, v. D-2, p. 261–306.
- Galley, J. D., 1958, Oil and gas geology in the Permian Basin in Texas and New Mexico, *in* Weeks, L. G., ed., Habitat of oil—a symposium: Tulsa, Oklahoma, American Association of Petroleum Geologists, p. 395–446.

Gass, T. E., 1982, The geothermal heat pump: Geothermal Resources Council Bulletin, v. 11, no. 11, p. 3–8.

Geothermal Survey of North America, 1970, Geothermal gradient maps of North America, Sheet 13 Central and west Texas and accompanying text, American Association of Petroleum Geologists, Tulsa, Oklahoma.

Harrison, W. E., Luza, K. V., Prater, M. L., and Cheung, P. K., 1983, Geothermal resource assessment in Oklahoma: Oklahoma Geological Survey Special Publication 83-1, 42 p.

Kehle, R. O., Schoepel, R. J., and Deford, R. K., 1970, The AAPG Geothermal Survey of North America, *in* United Nations Symposium on the Development and Utilization of Geothermal Resources, Proc., Vol. 2, Part 1.: Geothermics Special Issue 2, p. 358–367.

Ruppel, S.C., 1985, Stratigraphy and petroleum potential of pre-Pennsylvanian rocks, Palo Duro Basin, Texas Panhandle: The University of Texas at Austin, Bureau of Economic Geology Report of Investigations No. 147, 81 p.

Schoepel, R. J., Kehle, R. O., and Horn, M. K., 1970, Geothermal survey of North America: Second Annual Report, Report to American Association of Petroleum Geologists, October 1, 1970, 71 p.

Texas Water Development Board, 1972, A Survey of the subsurface saline water of Texas, v. 1, 113 p.

Woodruff, C. M., Jr., 1982, Geothermal resources of Texas: The University of Texas at Austin, Bureau of Economic Geology, Energy and Mineral Resources Map 3.

Wright, W. F., 1979, Petroleum geology of the Permian Basin: West Texas Geological Society Publication No. 79-71, 98 p.

APPENDIX (IN POCKET): DATA CD

Pdf of report

GIS_CD

Readme file

Metadata for GIS shapefiles

Data tables

Permian_basin_GIS_project.apr

Deliverables

Basement Structure Map

Precambrian_structure_ftssea_cont.shp

TectonicMap_wells_Precambrian.shp

Precambrian_wells.shp

TectonicMap_basement_faults.shp

TectonicMap_Precambrian_subcrop.shp

State_boundary.shp

County_boundary.shp

Permian_basin_study_area.shp

Geothermal Gradient Map

Geothermal_grad_smooth_cont.shp

Geothermal_grad_nosmooth_cont.shp

Geothermal_wells.shp

State_boundary.shp

County_boundary.shp

Permian_basin_study_area.shp

Supplementary Material

Ellenburger Structure Map

Ellenburger_structure_ftssea_cont.shp

TectonicMap_wells_Ellenburger.shp

TectonicMap_basement_faults.shp

TectonicMap_Precambrian_subcrop.shp

State_boundary.shp

County_boundary.shp

Permian_basin_study_area.shp

Digitized Tectonic Map data

TectonicMap_Ellenburger_structure_ftssea_cont.shp

TectonicMap_SiluroDev_structure_ftssea_cont.shp

TectonicMap_wells_Ellenburger.shp

TectonicMap_wells_SiluroDev.shp

TectonicMap_basement_faults.shp

TectonicMap_Precambrian_subcrop.shp

State_boundary.shp

County_boundary.shp

Permian_basin_study_area.shp